


 Cite this: *RSC Adv.*, 2025, 15, 43941

# The impact of phase modification on the equilibrium and kinetics of lanthanide(III) extraction from nitric acid media by TODGA

 Wyatt S. Nobley <sup>a</sup> and Mark P. Jensen <sup>\*ab</sup>

Organic phase modification is a commonly implemented strategy to avoid third phase formation in f-element solvent extraction. For trivalent lanthanide extraction by neutral extractants in alkane diluents, such as *N,N,N',N'*-tetra(*n*-octyl)diglycolamide (TODGA) in *n*-dodecane, the addition of a phase modifier is necessary to operate at high organic acid and metal loadings. Phase modifiers such as tri(*n*-butyl) phosphate (TBP) and *N,N*-di(*n*-hexyl)octanamide (DHOA) have been proven to be effective at preventing organic phase splitting well beyond the critical concentrations that limit the TODGA/*n*-dodecane phase without any modifiers. While the extraction capacity and loading limits of lanthanide extraction from nitric acid media by TODGA in alkane diluents have been evaluated for DHOA- and TBP-modified phases, the fundamental bulk equilibrium and kinetic mass transfer processes have not been well characterized for these systems. Solvent extraction and *operando* absorption spectroscopy were used to evaluate the impacts of DHOA and TBP on the equilibrium complexation and the reaction orders with respect to the extractant and acid. Compared to the unmodified organic phase, we determined that DHOA has very little effect on both the metal complexation and the interfacial kinetic mechanism. DHOA appears to act as a cosolvent, as phase modifiers are traditionally intended. In contrast, the addition of TBP to TODGA in *n*-dodecane altered the bulk TODGA:lanthanide(III) speciation and distinctly changed the transition state complex during reversible phase transfer of the cation between the aqueous phase and the organic phase. These results are novel and provide significant insight into the fundamental parameters defining this relevant f-element extraction system.

 Received 28th August 2025  
 Accepted 22nd September 2025

DOI: 10.1039/d5ra06417a

[rsc.li/rsc-advances](https://rsc.li/rsc-advances)

## Introduction

Solvent extraction of lanthanides from mineral acid media is currently the most effective industrial strategy to separate these 15 elements from other elements and from one another.<sup>1,2</sup> Organic ligands bind with different affinities to each lanthanide due to the contraction of the ionic radius across the series.<sup>3–5</sup> Particular organic-soluble ligands, known as extractants, aid in solubilizing the metal cation in nonpolar organic diluents like alkanes and can be used to separate individual lanthanides. For adjacent lanthanide separation, the acidic organophosphorus extractants have been best-in-class extractants for many decades.<sup>6,7</sup> More recently, the neutral diglycolamide (DGA) extractants have proven competitive for intra-lanthanide separation efficiency,<sup>5,8</sup> especially for the most abundant lanthanides, while also being useful in the nuclear fuel cycle in the separations of lanthanide(III) from actinide(III).<sup>9</sup>

The most studied DGA, *N,N,N',N'*-tetra(*n*-octyl)diglycolamide (TODGA), can operate across a broad range of conditions,<sup>10</sup> has

excellent organic phase solubility,<sup>9,11</sup> binds and releases lanthanides with relative ease, is sufficiently resistant to degradation,<sup>12</sup> and is completely incinerable. Despite these favorable characteristics, TODGA often forms undesirable third phases in alkane diluents under relevant metal-separations conditions.<sup>13</sup> TODGA pulls water, acid, and counteranions into the organic phase along with the extracted metal cation. When the organic phase acidity or metal concentration are sufficiently high, the organic phase will undergo phase splitting because of the overload of polar solutes in the nonpolar organic diluent. The result is two organic phases, one consisting of mostly diluent and unbound extractant, and a denser phase of mostly aggregated complexes of extractants, metal cations, and polar species.<sup>14–16</sup> To avoid this deleterious phase splitting, the solvating power of the paraffinic diluent is augmented with a small, amphiphilic molecule known as a phase modifier (PM).<sup>17,18</sup> PMs create a more hospitable environment for the polar species being extracted, thereby increasing the concentration of polar solutes that the organic phase can hold before the onset of the third phase<sup>19</sup> and enhancing the throughput of the separations process.

The impacts of PMs on the fundamental parameters that characterize the TODGA–*n*-dodecane–lanthanide(III)–nitric acid

<sup>a</sup>Chemistry Department, Colorado School of Mines, Golden, Colorado, USA

<sup>b</sup>Nuclear Science and Engineering Program, Colorado School of Mines, Golden, Colorado, USA. E-mail: [mjensen@mines.edu](mailto:mjensen@mines.edu)


solvent extraction system have been reviewed but are not yet fully understood.<sup>20</sup> Significant research has been devoted to the modifiers tri(*n*-butyl)phosphate (TBP), *N,N*-di(*n*-hexyl)octanamide (DHOA), and 1-alcohols.<sup>8,17,19–29</sup> The nitric acid extraction, lanthanide(III) extraction and separation, and limits of loading have been mostly characterized for these PMS,<sup>19,30,31</sup> but questions still remain regarding the role of the modifier in the solvation of the polar species. An even more significant question exists; how do these surface active PMS affect the kinetics of mass transfer? A few studies have delved into the kinetics of TODGA extraction of trivalent lanthanides,<sup>32–36</sup> but only one has specifically focused on organic phase modification. One study investigated TODGA kinetics using hydrogenated tetrapropylene and 5 vol% 1-octanol as the organic solvent.<sup>35</sup> While it was shown that the 1-octanol cause significant changes in interfacial tension measurements when added to the alkane diluent, this study did not compare the kinetics between unmodified and modified organic phases. A recent investigation looked at TBP, DHOA, and 1-octanol and their influence on TODGA–lanthanide(III) solvent extraction kinetics for the first time, beyond time-to-equilibrium studies.<sup>36</sup> It was found that the addition of PMS decreased the rate of extraction in all cases, and they found reaction orders of one for the components studied (TODGA, Nd(III), HNO<sub>3</sub>) with and without PMS, despite the possibility for higher slopes under pseudo-first order conditions.

In this study, we investigated the extraction of Nd(III) from nitric acid media by TODGA in *n*-dodecane containing the phase modifiers DHOA or TBP. Metal distribution between phases was determined and used to inform the analysis and interpretation of the kinetics of Nd extraction. Rate constants for the mass transfer were obtained using an *operando* UV/Vis spectroscopy technique under highly-stirred tank conditions. By isolating and varying different components of the chemical system, we were able to investigate the ways in which DHOA and TBP alter the extraction equilibrium and kinetics compared to the unmodified *n*-dodecane phase, which we have previously characterized.<sup>37</sup> TBP plays a more direct role in the metal complexation than DHOA and leads to significantly faster rates of extraction. DHOA appears to be a cosolvent, as PMS are traditionally intended to function, but TBP functions as both a cosolvent and cosurfactant under relevant conditions. These findings have implications both on the bulk complexation and the kinetic mechanism.

## Experimental

### Materials

Deionized water (18.2 MΩ) from a Millipore Direct-Q purifier and concentrated nitric acid (ACS grade) were used in the preparation of all aqueous samples. A stock solution of 0.478 ± 0.004 M neodymium(III) nitrate prepared in our laboratory was diluted appropriately for all Nd containing aqueous phases. The *n*-dodecane (99%) was purchased from Fisher Scientific. TODGA (99+%)<sup>8</sup> and DHOA (99.5+%)<sup>38</sup> were synthesized from procedures adapted from prior reports. More details can be found in the SI. TBP (99.5+%) was purchased from Alfa Aesar and further purified through vacuum distillation. Its purity was verified by <sup>31</sup>P NMR.

### Solvent extraction

Aqueous phases were prepared volumetrically with known masses of Nd(NO<sub>3</sub>)<sub>3</sub> stock solution and nitric acid diluted in water. Organic phases were prepared volumetrically with known masses of TODGA, TBP, and DHOA diluted in *n*-dodecane. All organic phases were pre-equilibrated twice with an equal volume of aqueous phase containing the appropriate concentration of HNO<sub>3</sub> without Nd present. This ensured that metal extraction experiments would remain at constant aqueous acidity.

Extractions were performed in triplicate for all concentrations of TODGA, TBP, DHOA, and HNO<sub>3</sub> reported in this study. TODGA concentration dependence experiments used 0.00490 M Nd(III) and ranged from 0.060 to 0.40 M TODGA at a constant aqueous concentration of 0.50 M HNO<sub>3</sub> with either 0.25 M or 1.0 M TBP or DHOA in the organic phase. Acid dependence experiments also used 0.00490 M Nd(III) with aqueous nitric acid concentrations that ranged from 0.20 to 3.0 M HNO<sub>3</sub> with a constant organic phase TODGA concentration of 0.10 M and either 0.25 M or 1.0 M TBP or DHOA in the organic phase. TBP and DHOA dependences ranged from 0.10–1.0 M phase modifier at constant aqueous 0.50 M HNO<sub>3</sub> and 0.00490 M Nd(III) and constant 0.10 M TODGA in *n*-dodecane. Equal volumes of fresh, Nd(III) containing aqueous phase and pre-equilibrated organic phase were placed in vials and shaken vigorously for 10 min at 2200 rpm using a Benchmark Scientific Benchmixer Vortex Mixer. Samples were centrifuged for 5 min at 2200 rpm using a Eppendorf benchtop centrifuge. The phases were separated, and an aliquot of the aqueous phase was diluted to 5 or 10 mL in a volumetric flask with 2% HNO<sub>3</sub>.

### ICP-OES

Pre- and post-extraction aqueous phase samples were analyzed for Nd content using a PerkinElmer Avio 220 Max Inductively-Coupled Plasma Optical Emission Spectroscopy (ICP-OES) instrument. The 406.109 and 401.225 nm emission bands were counted in both axial and radial viewing modes for each sample, and the counts were converted to Nd concentration through a 5-point calibration curve spanning 0–20 ppm Nd. Experimental error at 2σ was propagated through the calculations and accounted for in OriginPro linear regression fitting.

The equilibrium distribution ratio, defined as the ratio of concentrations of metal in the organic phase to aqueous phase at equilibrium, was calculated from aqueous phase measurements according to eqn (1), where *i* denotes initial and *eq* denotes equilibrium.

$$D_{\text{Nd}} = \frac{[\text{Nd}]_i - [\text{Nd}]_{\text{eq}}}{[\text{Nd}]_{\text{eq}}} \quad (1)$$

### Single-phase UV/visible absorption spectroscopy

Spectra were collected using a Varian Cary 5E spectrophotometer. Using a 1.000 cm pathlength quartz cuvette, post-extraction equilibrium organic phases were analyzed across



the wavelength range of 650–500 nm, which encompasses the  $^4I_{9/2} \rightarrow ^4G_{5/2}$ ,  $^2G_{7/2}$  hypersensitive electronic transitions of Nd(III). These transitions are sensitive to changes in the metal coordination environment. Organic phases contained varying concentrations of TODGA, DHOA, or TBP in *n*-dodecane, having been contacted with either 0.005 or 0.010 M Nd(III) in 0.50 M HNO<sub>3</sub>. ICP-OES analysis allowed for the determination of the Nd(III) concentration; therefore, the spectra were normalized to the molar absorptivity scale according to the Beer–Lambert Law for comparison. The number of unique light-absorbing species was identified from the spectral changes across a range of solution compositions using the programs SIXPack<sup>39</sup> and MCR-ALS,<sup>40,41</sup> and the equilibrium constants were calculated using the program SQUAD.<sup>42</sup>

### Kinetic experiments

Kinetic experiments were conducted using the Olis RSM 1000 DeSa Rapid-Scanning Monochromator Spectrophotometry System with CLARiTY attachment and a custom-made, overhead, two-blade stirrer. This configuration of the instrument uses a spinning disk with 16 slits and a dual monochromator setup to allow a ~70 nm wavelength range to pass through the sample at a maximum rate of 1 scan per 10 ms. The CLARiTY attachment includes an 8 mL round-bottom cell surrounded by a reflective coating, which boosts the pathlength and absorbance. Equal volumes (3.95 mL) of aqueous and organic phase were placed in the cell, then the overhead stirrer was carefully lowered into the cell, reaching to the interface between the phases. Data was collected for 50 s at 3.1 scans per s while stirring at 57 rpm, and the cell temperature was held at 22 ± 0.5 °C.

The three-dimensional raw kinetic data (wavelength, absorbance, time) were baseline corrected and two observable neodymium-containing species were identified using singular value decomposition in the Olis GlobalWorks software. The 2 Species Sequential Global Kinetic Fit provided an initial observed rate constant  $k_{\text{obs}}$  from which initial rate constants for the forward,  $k_{\text{ao}}$  (aqueous → organic, extraction), and reverse,  $k_{\text{oa}}$  (organic → aqueous, stripping), directions were obtained according to eqn (2) and (3). By incorporating the specific interfacial area ( $A/V$ ) into eqn (3), these relative observed rate constants, which depend on the interfacial area, are made absolute.

$$D_{\text{Nd}} = \frac{[\text{Nd}]_{\text{eq}}}{[\text{Nd}]_{\text{eq}}} = \frac{k_{\text{ao}}}{k_{\text{oa}}} \quad (2)$$

$$k_{\text{obs}} = \left(\frac{A}{V}\right)(k_{\text{ao}} + k_{\text{oa}}) \quad (3)$$

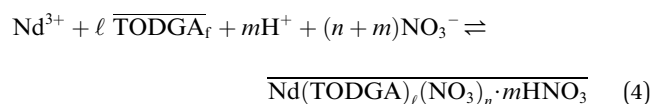
The specific interfacial area is the interfacial area ( $A$ , cm<sup>2</sup>) divided by the volume of the dispersed phase ( $V$ , cm<sup>3</sup>). Images of the stirred phases were acquired, randomly sampled, and analyzed across 0.10 to 1.0 M TBP and 0.10 to 1.0 M DHOA with constant 0.10 M TODGA, 0.50 M HNO<sub>3</sub>, and 4.90 mM Nd(III). The specific interfacial area was independent of TODGA and

HNO<sub>3</sub> concentrations but varied significantly with the concentration of phase modifier. These initial  $k_{\text{ao}}$  and  $k_{\text{oa}}$  values were input into the GlobalWorks Reversible First Order Global Kinetic Fit to obtain pseudo-first order forward and reverse rate constants.

## Results and discussion

### Effect of *N,N*-di(*n*-hexyl)octanamide (DHOA) on equilibrium and kinetics

Multiple monoamides have been examined as PMs for lanthanide(III) extraction by TODGA, and DHOA was identified as the best candidate. While DHOA extracts significant quantities of nitric acid,<sup>18,27</sup> it also prevents third phase effectively,<sup>18,19,27</sup> but its specific role in the extraction process is not understood. The general equilibrium for this extraction system is provided in eqn (4), which leads to the equilibrium constant  $K_{\text{ex}}$  defined in eqn (5). Using the distribution ratio defined in eqn (1) and taking the logarithm of eqn (5), rearrangement reveals a logarithmic dependence  $D_{\text{Nd}}$  on the TODGA concentration in eqn (6).



$$K_{\text{ex}} = \frac{[\overline{\text{Nd}(\text{TODGA})_\ell(\text{NO}_3)_n \cdot m\text{HNO}_3}]}{\{\text{Nd}^{3+}\} [\overline{\text{TODGA}}]_f^\ell \{\text{NO}_3^-\}^{n+m} \{\text{H}^+\}^m} \quad (5)$$

$$\log D_{\text{Nd}} = \ell \log [\overline{\text{TODGA}}]_f + \log((K_{\text{ex}})(\gamma_{\text{Nd}})\{\text{NO}_3^-\}^{n+m} \{\text{H}^+\}^m) \quad (6)$$

Equilibrium equations are functions of the activities of the species involved, but these are often approximated as concentrations. That approximation only holds at dilute concentrations of the species, thus the activity of aqueous Nd<sup>3+</sup>, NO<sub>3</sub><sup>−</sup>, and H<sup>+</sup> were used in this treatment due to the wide range of ionic strengths studied. The mean activity coefficients ( $\gamma_{\pm} = \gamma_{\text{NO}_3^-} = \gamma_{\text{H}^+}$ ) for aqueous species used herein were calculated using empirical models from previous studies,<sup>43–45</sup> while the activity coefficients of the organic phase species were assumed to be unity. The partial dissociation of HNO<sub>3</sub> in the aqueous phase was treated using previously measured values for the acid dissociation constant.<sup>44,45</sup> Free extractant ( $\overline{\text{TODGA}}_f$ ) was included to account for the loss of extractant to the cation and nitric acid.

Holding the acidity constant, the slope of the logarithmic plot of the  $D_{\text{Nd}}$  dependence on the  $\overline{\text{TODGA}}_f$  concentration in eqn (6) leads to the value  $\ell$ , which corresponds to the average number of extractant molecules coordinated to the metal in the bulk organic phase. While integer numbers are often expected for  $\ell$ , non-integer values are commonly found for TODGA: lanthanide complexation. These are usually explained as arising from a mixture of different complexes with different stoichiometries. For TODGA in unmodified *n*-dodecane extracting



Eu(III) from 1 M HNO<sub>3</sub>, literature values of  $\ell$  average 3.80, which implies a mixture of TODGA : Eu(III) complexes with 3 : 1 and 4 : 1 stoichiometry.<sup>20</sup> Although slope analysis can only provide an average stoichiometry and cannot eliminate the possibility of more polydisperse mixtures, studies have shown that the 3 : 1 homoleptic TODGA : Ln(III) complex dominates in these systems, and the association of any additional TODGA molecules likely occurs in the outer sphere of the complex where the TODGA is not coordinated to the cation directly.<sup>46–50</sup>

The extraction of Nd(III) from 0.50 M HNO<sub>3</sub> by 0.060–0.40 M TODGA dissolved in *n*-dodecane with either 0.25 M or 1.0 M DHOA yielded  $D_{\text{Nd}}$  values that increased with increasing TODGA concentrations, shown in Fig. 1. Error bars that were smaller than the point are not displayed but were included as weights in the fitting. Throughout the results presented in this study, data for the unmodified organic phase are included for comparison, which were collected and reported in a previous manuscript.<sup>37</sup> It is evident from an initial inspection of Fig. 1 that the addition of DHOA to the organic phase decreased the amount of Nd(III) extracted at equilibrium compared to the unmodified case. This occurred across all TODGA concentrations for both 0.25 M DHOA (9 vol%) and 1.0 M DHOA (36 vol%). The data in Fig. 1 is plotted as the logarithm of  $D_{\text{Nd}}$  versus the logarithm of organic TODGA concentration according to eqn (6), and the linear regressions fit well for each organic phase composition, with slopes reported in Table 1. There was no significant difference observed between slopes for unmodified *n*-dodecane ( $3.33 \pm 0.05$ ) and either 0.25 M DHOA ( $3.23 \pm 0.09$ ) or 1.0 M DHOA ( $3.41 \pm 0.14$ ). These results imply that DHOA does not compete with TODGA for metal coordination at equilibrium in the bulk organic phase and likely does not significantly alter the presence of any outer-sphere TODGA molecules.

In order to confirm that the TODGA complexation remains essentially unchanged at different DHOA concentrations, the

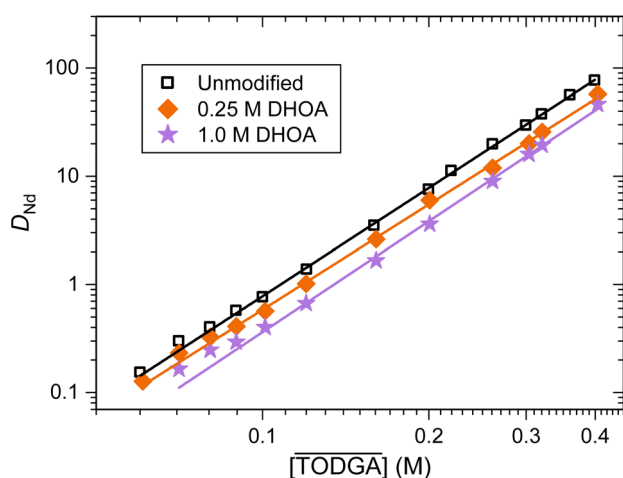


Fig. 1 Equilibrium distribution ratios for the extraction of 4.90 mM Nd(III) from 0.50 M HNO<sub>3</sub> by 0.060 to 0.40 M TODGA in *n*-dodecane without and with DHOA as a phase modifier. No phase modifier (black squares),<sup>37</sup> 0.25 M DHOA (orange diamonds), and 1.0 M DHOA (purple stars). Error bars ( $\pm 2\sigma$ ) smaller than their data point have been removed for clarity.

equilibrium Nd(III) complexes in the organic phase were examined spectroscopically across several DHOA and TODGA concentrations to examine the coordination environment around the extracted Nd cations (Fig. 2). Despite the wide range of DHOA concentrations studied (0–1.0 M), the shape of the spectra in Fig. 2A remained consistent. From no DHOA to 0.10 M DHOA an increase in the molar absorptivity was observed, but only a minor change was observed in the peak at 587 nm, which decreases from a distinct peak into a shoulder with increasing concentration of DHOA. Similarly, in Fig. 2B, addition of 1.0 M DHOA broadened the main peak at 583 nm for the lower TODGA concentrations. The features at 576 and 587 nm became significantly more distinct as the TODGA concentration was increased. Such spectral changes have been observed previously for the  $^4I_{9/2} \rightarrow ^4G_{5/2}, ^2G_{7/2}$  hypersensitive electronic transitions of Nd(III).<sup>51,52</sup> Campbell and coworkers observed a single peak at 583 nm with minor shoulders when a similar DGA extracted Nd(III) from 3 M NaNO<sub>3</sub>.<sup>51</sup> The addition of HNO<sub>3</sub> to the organic phase sharpened the features, leading to a crown-shaped spectrum similar to that in Fig. 2. Peroutka and coworkers observed the same phenomenon using TODGA.<sup>52</sup> They isolated the post-extraction organic phase from containing significant quantities of HNO<sub>3</sub>, which changed the hypersensitive band significantly and diminished the side peaks into shoulders of the main peak. We can interpret the variations in the spectrum for the 0.10 M TODGA + 1.0 M DHOA in *n*-dodecane system in Fig. 2B as being caused by interactions between DHOA and outer-sphere HNO<sub>3</sub>. It is well known that the association of water, nitrate, and nitric acid in the outer sphere of DGA complexes is extremely important to the extraction.<sup>46,47,53</sup> While DHOA does not appear to coordinate to the metal center or significantly disrupt TODGA in the interfacial mechanism (*vide infra*), the PM could interact with HNO<sub>3</sub> and disrupt hydrogen bonding in the outer sphere. A disruption of the interactions between the associated acid and the complex could lead to a broadening of the feature across 570–590 nm that changes the crown shape into a single peak with shoulders and likely decreases extraction (Fig. 1). Greater concentrations of TODGA, such as 0.30 and 0.40 M, were able to outcompete this effect of DHOA in the outer sphere, reforming the crown-shaped spectrum (Fig. 2B).

DHOA has been proposed as a possible lanthanide(III) coextractant with TODGA,<sup>54</sup> but this claim has not been verified, and the slope analysis presented in Fig. 1 and Table 1 indicate that DHOA acts primarily as a cosolvent. DHOA antagonizes the extraction because it extracts significantly more acid and water into the organic phase. While it aids in solubilizing the extracted complexes at higher loadings to prevent third phase,<sup>18,27</sup> DHOA does not provide more stable complexes by binding the cation. It is possible that the observed antagonism toward lanthanide(III) extractability is caused by DHOA–HNO<sub>3</sub>–H<sub>2</sub>O–TODGA interactions, which would lower the amount of TODGA available for binding the metal. Developing a full picture of the post-extraction, phase-modified organic phase, however, will require spectroscopic and computational investigations on the interplay between extractant, acid, and DHOA modifier.



**Table 1** Slopes of the linear regression fits for the dependence (dep) of  $D_{\text{Nd}}$ ,  $k_{\text{ao}}$ , and  $k_{\text{oa}}$  on the TODGA concentration and aqueous nitrate anion activity for unmodified *n*-dodecane<sup>37</sup> and solutions modified with 0.25 M and 1.0 M DHOA. Uncertainties are reported at  $\pm 2\sigma$  from an error-weighted linear regression

Phase modifier	$D_{\text{Nd}}$ dep on [TODGA]	$k_{\text{ao}}$ dep on [TODGA]	$k_{\text{oa}}$ dep on [TODGA]	$k_{\text{ao}}$ dep on $\{\text{NO}_3^-\}$	$k_{\text{oa}}$ dep on $\{\text{NO}_3^-\}$
Unmodified	$3.33 \pm 0.05$	$2.97 \pm 0.05$	$-3.14 \pm 0.20$	$2.17 \pm 0.13$	$-3.63 \pm 0.14$
0.25 M DHOA	$3.23 \pm 0.09$	$2.86 \pm 0.28$	$-2.78 \pm 0.22$	$2.80 \pm 0.07$	$-3.44 \pm 0.35$
1.0 M DHOA	$3.41 \pm 0.14$	$2.97 \pm 0.09$	$-2.85 \pm 0.09$	$3.14 \pm 0.13$	$-2.82 \pm 0.24$

In order to understand the effect of DHOA on the mass transfer kinetics of Nd(III) partitioning between nitric acid media and TODGA in *n*-dodecane, *operando* optical spectroscopy and 3-dimensional data fitting were performed as described above. Both  $k_{\text{ao}}$  (aqueous  $\rightarrow$  organic) and  $k_{\text{oa}}$  (organic  $\rightarrow$  aqueous) pseudo-first order rate constants are functions of the components in the system,<sup>55</sup>

$$k_{\text{ao}} = f_1 \left( [\text{TODGA}]_f^a, \{\text{NO}_3^-\}^b, [\text{DHOA}]^c \right) \quad (7)$$

$$k_{\text{oa}} = f_2 \left( [\text{TODGA}]_f^d, \{\text{NO}_3^-\}^e, [\text{DHOA}]^f \right) \quad (8)$$

and the order with respect to each reactant can be determined by taking the logarithm of both sides, shown in eqn (9) as an example.

$$\log k_{\text{ao}} = a \log [\text{TODGA}]_f + \log \left( \{\text{NO}_3^-\}^b [\text{DHOA}]^c \right) \quad (9)$$

Plotting  $k_{\text{ao}}$  versus TODGA concentration on a logarithmic scale, while holding other components constant, should lead to an interpretable slope  $a$ , which in eqn (9) is the order of the reaction with respect to TODGA.

Kinetic experiments were performed from 0.060 to 0.40 M TODGA at a constant aqueous concentration of 0.50 M HNO<sub>3</sub> and an initial aqueous concentration of 4.90 mM Nd(III). An example of the spectra collected during the extraction of Nd(III) in the 0.12 M TODGA + 1.0 M DHOA in *n*-dodecane system is provided in Fig. 3A. These conditions gave an equilibrium  $D_{\text{Nd}}$  of 0.67 and a  $k_{\text{obs}}$  of  $0.188 \text{ s}^{-1}$  (corrected for the specific interfacial area,  $k_{\text{obs}} = 5.47 \times 10^{-4} \text{ cm s}^{-1}$ ). Fig. 3B tracks the absorbances of the most prominent wavelengths as they evolved over time, with every other point removed for clarity. Since the round bottom cell holds both phases while they are vigorously stirred, these spectra represent a combination of the Nd(III) hypersensitive band for aqueous and organic bulk complexation. The peak centered at 576 nm was prominent in both phases, so it initially decreased, then increased smoothly like the peaks at 583 nm and 587 nm.

The resulting rate constants are provided in Fig. 4. In the forward direction (Fig. 4A), the addition of 0.25 M DHOA to *n*-dodecane had almost no effect on  $k_{\text{ao}}$ , but it hastened the rate of stripping (Fig. 4B) for the higher TODGA concentrations. Quadrupling the DHOA concentration, on the other hand, slowed extraction ( $k_{\text{ao}}$ ) by approximately a factor of 3 across the lowest TODGA concentrations. The rate constants for the reverse reaction,  $k_{\text{oa}}$ , were nearly identical to those of the 0.25 M

DHOA system. Furthermore, the data in Fig. 4 exhibit linear regions at low TODGA concentrations and high TODGA concentrations for  $k_{\text{ao}}$  and  $k_{\text{oa}}$ , respectively. While the curvature of these plots implies that the mechanism of extraction and stripping are complex, like that observed for TODGA in the unmodified system,<sup>37</sup> the slopes of the linear regions provide the limiting reaction order for the rate law with respect to TODGA (Table 1). It is evident that the rate law remains unchanged with respect to TODGA when DHOA is used as a phase modifier. The statistically similar slopes, along with the

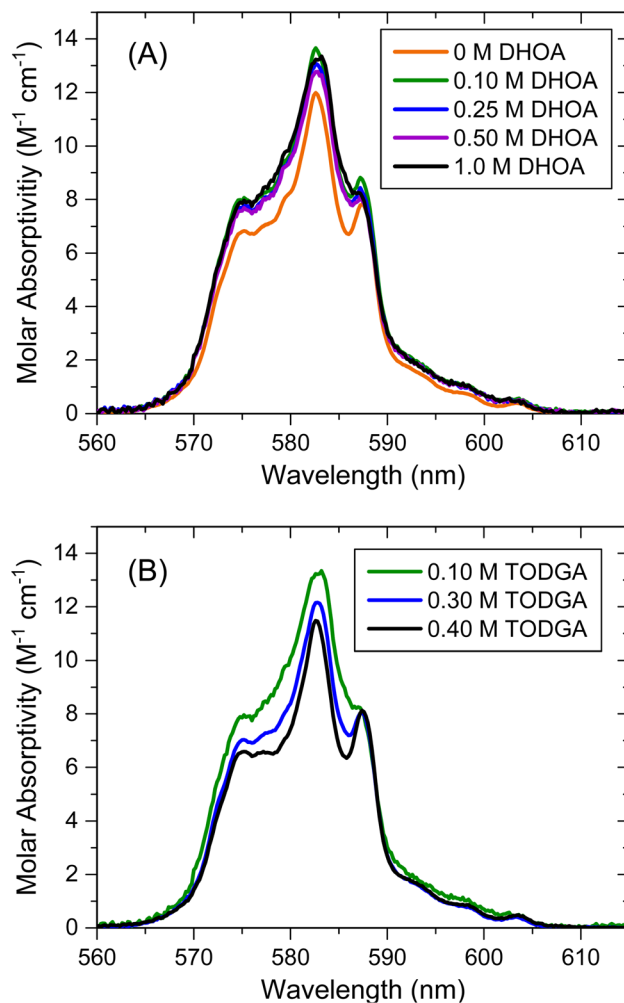


**Fig. 2** Molar absorptivities of Nd(III) after extraction by TODGA in *n*-dodecane containing DHOA as a phase modifier. Organic: (A) 0.10 M TODGA + 0, 0.10, 0.25, 0.50, or 1.0 M DHOA in *n*-dodecane, and (B) 1.0 M DHOA + 0.10, 0.30, or 0.40 M TODGA in *n*-dodecane.



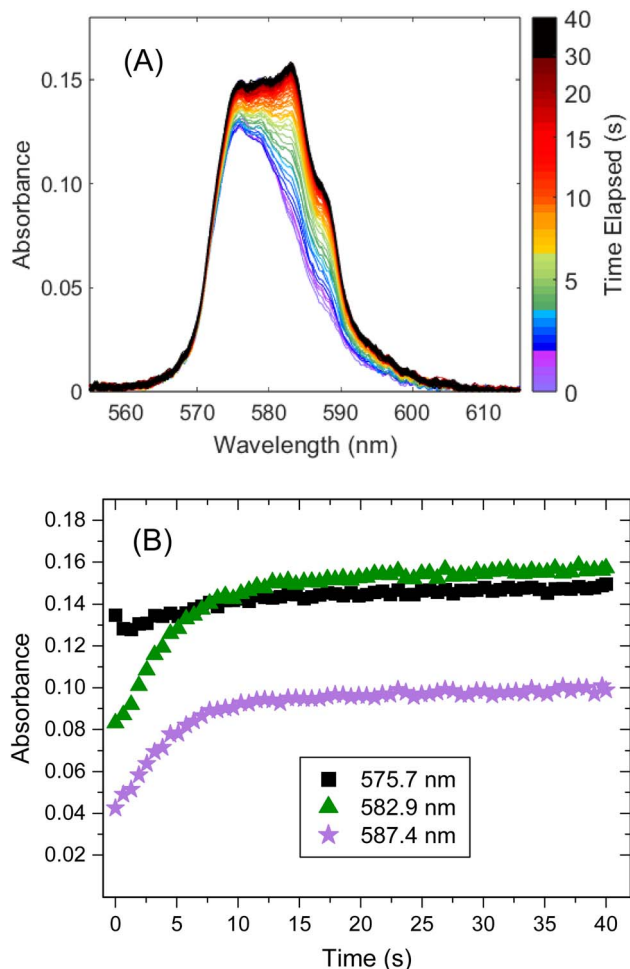


**Fig. 3** Example of the data collected using the Olis RSM with CLARITY and overhead stirrer. (A) Spectra collected over 40 s while 4.90 mM Nd(III) in 0.50 M HNO<sub>3</sub> was extracted by 0.12 M TODGA + 1.0 M DHOA in *n*-dodecane. (B) Absorbances of the three main peaks of the spectra as they evolve over time, with every other data point removed for clarity.

similarly shaped curves, indicate that the mechanism of mass transfer with respect to TODGA is the same as previously described for the unmodified organic phase.<sup>37</sup> After a slow step where Nd(III) adsorbs at the interface, being bound by an initial TODGA extractant, two additional TODGA molecules associate with the metal before the complex (with nitrate anions) desorbs from the interface in a second slow step. In the reverse direction, all three TODGA molecules dissociate from the complex before the cation transfers across the interface and returns to the aqueous phase, likely with the release of the final bound TODGA being the slow desorption step.

Dependencies of  $D_{\text{Nd}}$ ,  $k_{\text{ao}}$ , and  $k_{\text{oa}}$  across DHOA concentrations (0.10 to 1.0 M) at constant 0.10 M TODGA and 0.50 M HNO<sub>3</sub> are provided in Fig. S1. The results are consistent with the discussion thus far, since an increase in the concentration of DHOA decreased the degree of extraction at equilibrium, slowed the forward rate, and had almost no effect on the reverse rate. Meaningful slopes were not obtained from the changes in

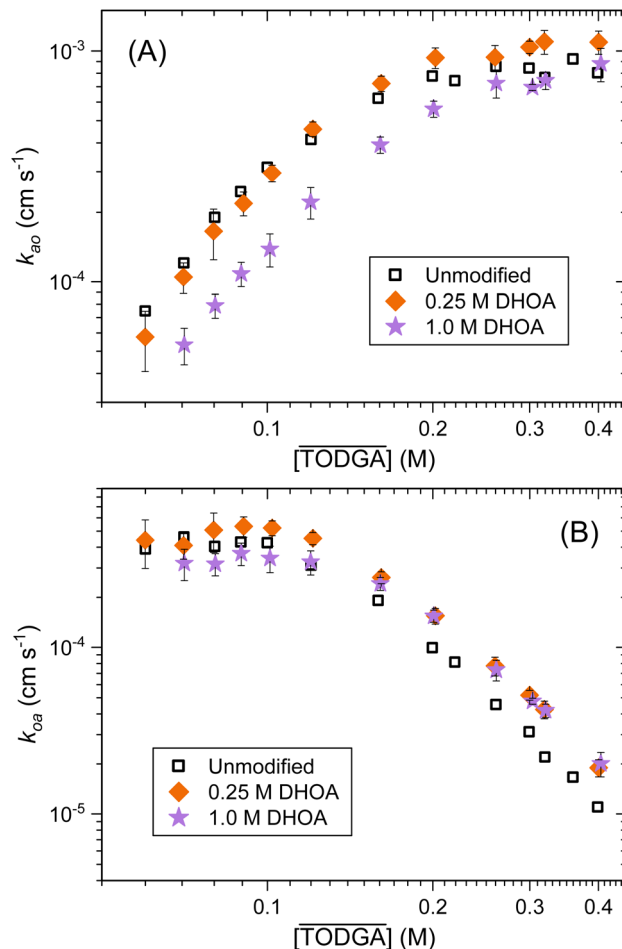


**Fig. 4** Pseudo-first order rate constants for the (A) aqueous to organic and (B) organic to aqueous mass transfer of Nd(III) by 0.060 to 0.40 M TODGA in *n*-dodecane without and with DHOA as a phase modifier. The equilibrium aqueous phase acidity was 0.50 M HNO<sub>3</sub>. No phase modifier (black squares),<sup>37</sup> 0.25 M DHOA (orange diamonds), and 1.0 M DHOA (purple stars). Error bars are provided at  $\pm 2\sigma$ .

DHOA concentration, and despite its role as an f-element extractant, DHOA does not alter the complexation of TODGA with the trivalent lanthanide. The role of DHOA in slowing down the forward kinetics is likely due to its presence at the interface without providing any new mechanisms for transfer. Since DHOA appears to not interact with the metal, it would only compete with TODGA adsorbed at the interface and slow down the rate at which three TODGA molecules can bind to the metal or free TODGA molecules can displace the metal-TODGA complex from the interface so that the complex can transfer into the organic phase.

Even though the presence of DHOA did not affect the TODGA complexation to Nd, the spectroscopic evidence in Fig. 2B suggests that the modifier interacts with HNO<sub>3</sub> in the outer sphere of the organic phase complexes. In order to investigate these potential interactions between DHOA and nitrate species, we studied the effect of DHOA modification across a range of aqueous equilibrium HNO<sub>3</sub> concentrations on the thermodynamic and kinetic parameters described thus far. As the



aqueous acidity was varied from 0.20–3.0 M HNO<sub>3</sub>, the Nd(III) concentration was held at 4.90 mM, and the TODGA concentration was held at 0.10 M with either 0.25 M or 1.0 M DHOA in *n*-dodecane. Due to the wide range of HNO<sub>3</sub> concentrations used, it was necessary to account for the nitrate anion activity,<sup>44</sup> {NO<sub>3</sub><sup>-</sup>}, to understand the dependence of the distribution ratio and rate constants on nitrate species.

The resulting logarithmic dependence of  $D_{\text{Nd}}$  on {NO<sub>3</sub><sup>-</sup>} is provided in Fig. 5. Due to the nonlinear curves in Fig. 5, eqn (6) cannot be directly applied to this data, and a more in-depth fitting would be needed to fully understand the nitrate anion and nitric acid contributions to  $D_{\text{Nd}}$ .<sup>37</sup> This was executed for the unmodified data in our previous work, but requires knowledge of the organic phase composition, such as the extraction of nitric acid and the free extractant concentration. That data is not available for DHOA-modified organic phases, but the relative changes that occurred in the acid dependence results provide certain insights into the impact of DHOA on the equilibrium and kinetics.

The addition of DHOA led to lower extraction, slower extraction, and faster stripping across almost all acidities tested. Interestingly, the equilibrium distribution ratios tailed off at the highest acidities when 0.25 M DHOA was in the organic phase, and this effect was significantly enhanced when the DHOA concentration was quadrupled (Fig. 5). It is evident that the modifier, which is known to increase the solubility of aggregates and prevent third phase formation, decreases the stability and solubility of the Nd(III) complexes relative to the unmodified organic phase. Alkane diluents consistently foster greater extraction of metal by TODGA than most polar diluents.<sup>20</sup> The 3 : 1 (often 4 : 1) TODGA : Ln(III) complex is highly favorable in alkane diluents. The creation of significant polarity in the organic phase, whether by changing the diluent or adding a PM, likely disrupts alkyl chain overlap, alters the outer-sphere

interactions, and reduces the amount of TODGA that is free to bind the metal.

The impact of changing the aqueous acidity, and thus the nitrate anion activity, on  $k_{\text{ao}}$  and  $k_{\text{oa}}$  are depicted in Fig. 6. Limiting linear regions were observed in the kinetic data, and the slopes of these linear regions are provided in Table 1. In the forward direction, the initial slope increased in the order 2.2, 2.8, and 3.1 for 0, 0.25, and 1.0 M DHOA, respectively.

In order to understand this change, it is necessary to consider the unmodified system in more detail. It is known that three nitrate anions accompany the trivalent metal cation into the bulk organic phase to retain charge balance. In our previous analysis of the unmodified organic phase, we determined that the changes in  $k_{\text{ao}}$  at low nitrate anion activities were completely accounted for by the changes in  $D_{\text{Nd}}$ , because of the plateau in  $k_{\text{oa}}$  values.<sup>37</sup> In that study, the unmodified  $D_{\text{Nd}}$  curve showed a slope across low {NO<sub>3</sub><sup>-</sup>} that was less than 3 due to the flattening of the curve to a baseline extraction where the

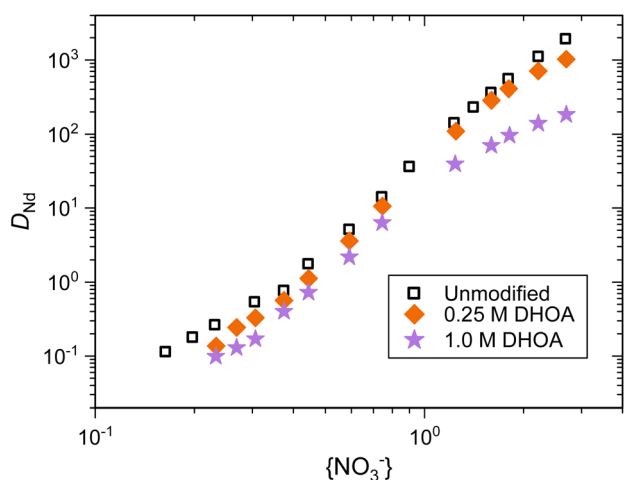


Fig. 5 Equilibrium distribution ratios for the extraction of 4.90 mM Nd(III) from 0.20 to 3.0 M HNO<sub>3</sub> by 0.10 M TODGA in *n*-dodecane without and with DHOA as a phase modifier. No phase modifier (black squares),<sup>37</sup> 0.25 M DHOA (orange diamonds), and 1.0 M DHOA (purple stars). Error bars ( $\pm 2\sigma$ ) smaller than their data point have been removed for clarity.

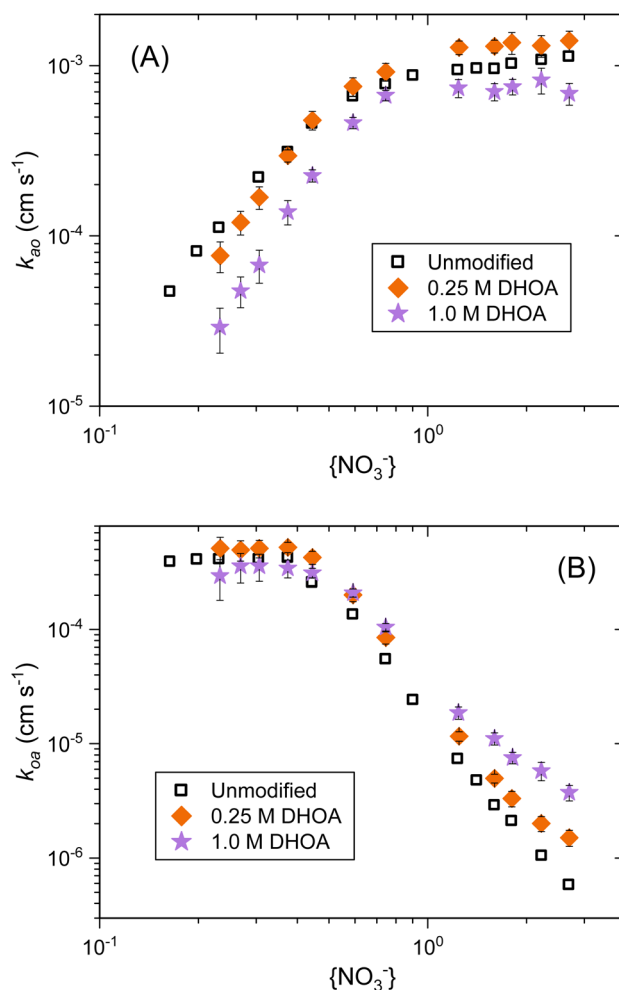


Fig. 6 Pseudo-first order rate constants for the (A) aqueous to organic and (B) organic to aqueous mass transfer of Nd(III) from 0.20 to 3.0 M HNO<sub>3</sub> by 0.10 M TODGA in *n*-dodecane without and with DHOA as a phase modifier. No phase modifier (black squares),<sup>37</sup> 0.25 M DHOA (orange diamonds), and 1.0 M DHOA (purple stars). Error bars are provided at  $\pm 2\sigma$ .



distribution becomes nearly independent of the acidity. When all aqueous-phase activities (including water, nitrate anions, protons, and the metal cation) and free TODGA corrections were applied to the distribution ratio curve, a slope of 3 was observed across this lower nitrate anion activity region. Since  $k_{\text{oa}}$  is unchanging across this region, we used the corrected  $D_{\text{Nd}}$  slope to interpret the  $k_{\text{ao}}$  values. Across the higher  $\{\text{NO}_3^-\}$  region, the  $k_{\text{ao}}$  curve reaches a plateau, and the corrected  $D_{\text{Nd}}$  curve reached a limiting slope of approximately 7. This nitrate dependence slope was applied to the slope in  $k_{\text{oa}}$  across the higher acidity region. Therefore, it was concluded that three nitrate anions are involved at or before the rate limiting adsorption to and desorption from the interface when Nd(III) is transferred from the aqueous phase to the organic phase. A slope magnitude of 7 across high nitrate anion activities in the unmodified organic phase stripping kinetics implied that three nitrate anions and two nitric acid adducts ( $2m + n = 7$ ) dissociated from the metal complex before the rate-limiting desorption of the cation into the aqueous phase.<sup>37</sup>

In light of this analysis for the unmodified extraction system, addition of DHOA as a phase modifier appears to impact the equilibrium and kinetics across the acidity range studied. Based on the nitrate activity slopes of 2.8 and 3.1 (0.25 M and 1.0 M DHOA) for  $k_{\text{ao}}$  across the low  $\{\text{NO}_3^-\}$  region (Fig. 6), DHOA shifts the baseline metal extraction to lower acidities, which causes the slopes of the  $D_{\text{Nd}}$  and  $k_{\text{ao}}$  plots to approach the ideal slope of 3 in the DHOA containing systems as compared to the phase modifier-free system. The increase of the slopes from 2.8 to 3.1 for 0.25 M and 1.0 M DHOA, respectively, confirms that this is a DHOA-based effect, likely due to the added polarity that the modifier affords the organic phase. Therefore, we can conclude that the aqueous to organic mass transfer kinetics are governed by the same mechanism with DHOA present as with no modifier, and three nitrate anions associate to the cation in fast equilibria before desorption into the organic phase.

Another impact of DHOA modification of the system is apparent in the stripping kinetics. While 0.25 M DHOA affected the slope at high aqueous nitrate activities to some extent, the presence of 1.0 M DHOA lowered the reaction order of  $k_{\text{oa}}$  with respect to nitrate to  $-2.8$  (Fig. 6B and Table 1). Relatively large standard deviations are associated with these slopes due to the curvature of the data as nitrate anion activity increases. This curvature is a result of the curvature in the uncorrected distribution ratios (Fig. 5) and the plateau in forward rate constants (Fig. 6A). Nevertheless, the decrease in the limiting slope in the stripping kinetics, the tailed-off  $D_{\text{Nd}}$  values in Fig. 5, and interactions of DHOA and  $\text{HNO}_3$  evident in the spectral changes in Fig. 2B, imply that DHOA has an impact on the outer-sphere  $\text{HNO}_3$  adducts in the Nd complex. The presence of DHOA may be displacing  $\text{HNO}_3$  from the organic phase Nd(III) complex, which would then remove  $\text{HNO}_3$  from the dissociative equilibria of the stripping mechanism. A much more extensive treatment of the data, with knowledge of the degree of acid and water extraction, aqueous activities, the free extractant concentration, and the extent of any interactions between DHOA and the Nd complexes would be necessary to verify this claim.

As a PM, the monoamide DHOA does not alter the equilibrium or the kinetic mechanism of lanthanide(III) extraction from nitric acid media by TODGA in *n*-dodecane to a significant extent. DHOA appears to be a cosolvent in the bulk organic phase, not interacting with the metal center, although it may interact with outer-sphere  $\text{HNO}_3$  adducts. In the kinetics, the data show that 1.0 M DHOA substantially decreases the forward rate across TODGA concentrations and acidities. Most likely, the DHOA amphiphile displaces some of the interfacial TODGA. Since the PM does not change the mechanism or enable alternative mechanisms for mass transfer, DHOA served to decrease the rate at which the TODGA extractants can bind to the metal at the interface.

### Effect of tri(*n*-butyl)phosphate (TBP) on equilibrium and kinetics

Many studies have investigated TBP as a PM for TODGA–lanthanide(III) extractions, with the majority of these studies focused on acid extraction and determining the limits of third phase formation with acid and metal.<sup>19,25,45,56</sup> The impact of TBP on distribution ratios, organic phase complexation, and kinetics were determined in this study following a similar experimental approach and analysis used for DHOA above.

DHOA and TBP are both monodentate, neutral ligands that are used for similar f-element separations, but when they are used as PMs for the extraction of lanthanide(III) cations by DGAs, they show opposite effects. As previously reported, TBP enhances the extent of lanthanide extraction<sup>24,56</sup> while DHOA generally decreases the amount of lanthanide extracted.<sup>18,27</sup> The resulting  $D_{\text{Nd}}$  values obtained across 0.060–0.40 M initial TODGA concentration with 0.25 M (6.8 vol%) or 1.0 M (27 vol%) TBP in *n*-dodecane are plotted on logarithmic scales in Fig. 7. The total TODGA concentration was corrected to the free

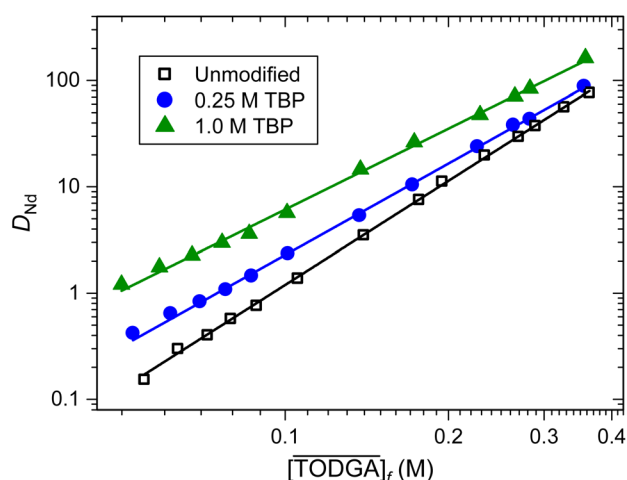


Fig. 7 Equilibrium distribution ratios for the extraction of 4.90 mM Nd(III) from 0.50 M  $\text{HNO}_3$  by 0.060 to 0.40 M TODGA in *n*-dodecane without and with TBP as a phase modifier. No phase modifier (black squares),<sup>37</sup> 0.25 M TBP (blue circles), and 1.0 M TBP (green triangles). Error bars ( $\pm 2\sigma$ ) smaller than their data point have been removed for clarity.



**Table 2** Slopes of the linear regression fits for the dependence (dep) of  $D_{\text{Nd}}$  on free TODGA concentration for unmodified *n*-dodecane<sup>37</sup> and modified with 0.25 M and 1.0 M TBP. Uncertainties are reported as  $\pm 2\sigma$  from error-weighted linear regression

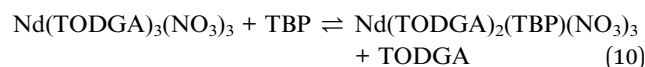
Phase modifier	$D_{\text{Nd}}$ dep on $[\text{TODGA}]_{\text{f}}$	$D_{\text{Nd}}$ dep at low $[\text{TODGA}]_{\text{f}}$	$D_{\text{Nd}}$ dep at high $[\text{TODGA}]_{\text{f}}$
Unmodified	$3.25 \pm 0.05$	$3.13 \pm 0.19$	$3.25 \pm 0.07$
0.25 M TBP	$2.86 \pm 0.05$	$2.43 \pm 0.13$	$2.90 \pm 0.06$
1.0 M TBP	$2.53 \pm 0.08$	$2.00 \pm 0.12$	$2.57 \pm 0.14$

TODGA concentration ( $[\text{TODGA}]_{\text{f}}$ ) using the nitric acid extraction data provided by McLachlan *et al.*<sup>45</sup> and the Nd(III) extraction results obtained in this work. The results for the TBP modified system show the opposite of the effect of DHOA modified system. The equilibrium extraction of Nd was significantly enhanced by TBP, even with only 0.25 M of the modifier present (Fig. 7). At the lowest TODGA concentrations, 1.0 M TBP modifier caused almost an order of magnitude increase in extraction compared to the unmodified extraction system. Despite its propensity to extract significant quantities of acid and water,<sup>25,45,56</sup> just like DHOA,<sup>18,20</sup> TBP is beneficial to the extraction of Nd(III) by TODGA.

The slopes for the linear regressions of the equilibrium data in Fig. 7 are provided in Table 2. Greater quantities of TBP ushered in distinct decreases in the magnitude of the equilibrium TODGA dependence slope. A slope of 2.86 for 0.25 M TBP, and a further decrease to 2.53 for 1.0 M TBP, indicates that the presence of TBP in the system reduces the average number of TODGA molecules bound to the Nd ions in the equilibrium organic phase complex. However, a more thorough analysis of the equilibrium extraction data from Fig. 7 shows some curvature of the data, and the  $D_{\text{Nd}}$  data for both the 0.25 M and 1.0 M TBP systems can be fit with two linear regions with distinct slopes (Fig. S2). This approach tracked the data well, and the resulting slopes are provided in Table 2. For both TBP concentrations, equilibrium complexes containing only two TODGA molecules were more prevalent in the bulk organic phase at the low, 0.060–0.10 M initial TODGA, concentrations. The number of coordinated TODGA molecules rose much closer to three when the TODGA concentration was increased beyond 0.12 M. This is a clear sign of competition between TODGA and TBP for metal coordination in the organic phase.

The TBP-modified experiments revealed a unique spectral signal that was investigated using conventional optical absorption spectroscopy. In the DHOA-modified experiments discussed above, the presence of DHOA did not alter the hypersensitive Nd(III) absorption band centered at 580 nm except to broaden the main peak (Fig. 2), which was indicative of interaction with  $\text{HNO}_3$  in the outer sphere. In contrast, the spectra from the TBP-modified system (Fig. 8) exhibited significant changes. A new peak appeared at 579 nm when TBP was introduced into the organic phase and grew larger with increasing concentrations of TBP (Fig. 8A). As the concentration of TODGA was increased while holding the TBP concentration constant at 1.0 M, the peak receded, and the spectra re-formed the familiar crown shape (Fig. 8B). Such results have not been reported before for this extraction system. The spectral changes across TBP concentrations were analyzed using the program,

SQUAD, and the best fitting model involved the exchange of one TBP for one TODGA by the equilibrium,



with an equilibrium constant of  $0.752 \pm 0.043$ . The SQUAD calculated spectra from the fit were consistent with the experimental spectra (Fig. S3) and reached an equilibrium where equal fractions of  $\text{Nd}(\text{TODGA})_3(\text{NO}_3)_3$  and

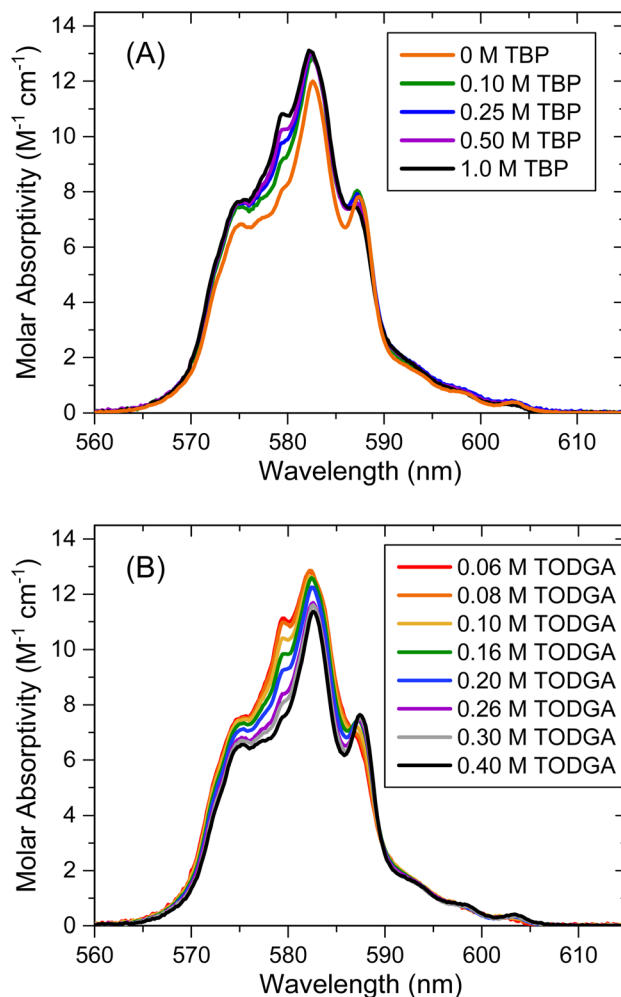


**Fig. 8** Molar absorptivities of Nd(III) after extraction by TODGA in *n*-dodecane containing TBP as a phase modifier. Organic phases were (A) 0.10 M TODGA + 0.10, 0.25, 0.50, or 1.0 M TBP in *n*-dodecane, and (B) 1.0 M TBP + 0.060 to 0.40 M TODGA in *n*-dodecane.



$\text{Nd}(\text{TODGA})_2(\text{TBP})(\text{NO}_3)_3$  were present in the organic phase just above 0.10 M TBP and 0.10 M TODGA (Fig. S4).

Based on the spectra in Fig. 8 and the  $D_{\text{Nd}}$  values reported in Fig. 7, TBP appears to be a synergist for Nd(III) extraction by TODGA in *n*-dodecane. TODGA, being the stronger trivalent lanthanide extractant, remains complexed to the Nd in a 2 : 1 TODGA:Nd ratio despite the excess of TBP in the organic phase, and forms the favorable 3 : 1 homoleptic complex at higher TODGA concentrations, which provides the triple-peaked spectrum shown in the black trace in Fig. 8B. As the TBP concentration was increased from 0–1.0 M with constant 0.10 M TODGA in *n*-dodecane, a new species formed that included one TBP molecule. Similarly, as the TODGA concentration was increased from 0.060–0.40 M at constant 1.0 M TBP, the coordinated TBP molecule was replaced and the species changed from  $\text{Nd}(\text{TODGA})_2(\text{TBP})(\text{NO}_3)_3(\text{HNO}_3)_{0-2}$  to the complex,  $\text{Nd}(\text{TODGA})_3(\text{NO}_3)_3(\text{HNO}_3)_{0-2}$  that is found in *n*-dodecane solutions. The significant increases in  $D_{\text{Nd}}$  provided by TBP-modification of the *n*-dodecane diluent, considering the

low  $D_{\text{Nd}}$  value of 0.05 when Nd(III) was extracted from 1 M  $\text{HNO}_3$  by 1.0 M TBP in *n*-dodecane without TODGA, prove TBP is not just competitive with TODGA for coordination but that it acts as a synergist in the extraction even at high TODGA concentrations when TBP is not directly coordinated to the lanthanide.

The pseudo-first order rate constants for forward ( $k_{\text{ao}}$ ) and reverse ( $k_{\text{oa}}$ ) mass transfer of Nd(III) were determined across the same range of total TODGA concentrations studied in the DHOA modified system. The results are shown as a function of free TODGA concentration on logarithmic scales in Fig. 9. Unlike either the DHOA-modified or the unmodified *n*-dodecane systems, the TBP-modified organic phases led to limiting TODGA reaction orders for  $k_{\text{ao}}$  that were significantly less than three (Table 3). Notably, the  $k_{\text{oa}}$  curve for the 1.0 M TBP system did not plateau at the lowest TODGA concentrations that were studied (Fig. 9B). In 1.0 M TBP, two linear regions exist with slopes of  $-1.11 \pm 0.08$  for the low  $[\text{TODGA}]_{\text{f}}$  region and  $-2.25 \pm 0.09$  for the higher concentration region. This change of the shape of the  $k_{\text{oa}}$  curve, along with the limiting TODGA reaction orders of 1.82 and 0.98 observed for the  $k_{\text{ao}}$  dependence using 0.25 M and 1.0 M TBP, respectively, signify significant changes in the extraction mechanism and rate laws defining mass transfer in both directions.

If we assume that the solvent extraction kinetics of the DHOA and TBP containing systems are governed by chemical reactions at the interface, just like the TODGA/*n*-dodecane system appears to be,<sup>37</sup> the TBP-modified kinetic results can be interpreted in terms of changes to the rate laws and chemical mechanisms of interfacial mass transfer. TBP speeds up the aqueous to organic phase transfer consistently across the lower TODGA concentration range. This is due to the altered mechanism that TBP induces for mass transfer across the interface, potentially lowering the activation barrier. Based on the slopes of the initial linear regions in the forward direction (Fig. 9A) reported in Table 3, only one TODGA molecule is coordinated to the metal in the transition state for the extraction in 1.0 M TBP-modified *n*-dodecane. Thus, the presence of 1.0 M TBP in the system removes two TODGA molecules from the activated complex in the rate limiting step(s) compared to the unmodified and DHOA modified systems. Considering that an average of 2.5 TODGA extractants are still bound to the complex in the bulk organic phase when 1.0 M TBP is present, it is clear that solvent modification by TBP has a greater effect on the kinetic mechanism than on the equilibrium speciation. This is consistent with the fact that TBP is active at the interface<sup>37,58</sup> (especially at when the bulk TBP concentration is 1.0 M) but is a weak extractant for trivalent lanthanides. The difference between the

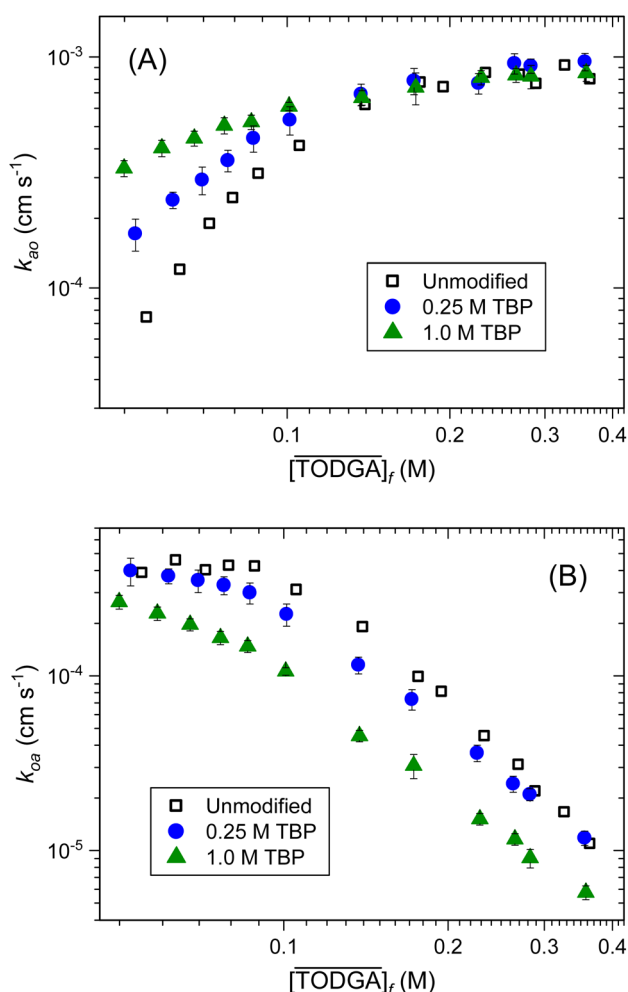


**Fig. 9** Pseudo-first order rate constants for the (A) aqueous to organic and (B) organic to aqueous mass transfer of Nd(III) by 0.060 to 0.40 M TODGA in *n*-dodecane without and with TBP as a phase modifier. The equilibrium aqueous phase acidity was 0.50 M  $\text{HNO}_3$ . No phase modifier (black squares),<sup>37</sup> 0.25 M TBP (blue circles), and 1.0 M TBP (green triangles). Error bars are provided at  $\pm 2\sigma$ .

**Table 3** Slopes of the linear regression fits for the dependence (dep) of  $k_{\text{ao}}$  and  $k_{\text{oa}}$  on free TODGA concentration for unmodified *n*-dodecane<sup>37</sup> and modified with 0.25 M and 1.0 M TBP. Error is reported as  $\pm 2\sigma$  from error-weighted linear regression

Phase modifier	$k_{\text{ao}}$ dep on $[\text{TODGA}]_{\text{f}}$	$k_{\text{oa}}$ dep on $[\text{TODGA}]_{\text{f}}$
Unmodified	$3.03 \pm 0.32$	$-3.01 \pm 0.18$
0.25 M TBP	$1.82 \pm 0.12$	$-2.42 \pm 0.08$
1.0 M TBP	$0.98 \pm 0.15$	$-2.25 \pm 0.09$



number of TODGA molecules involved in the transition state of the forward reaction as reflected in the kinetic rate law and the additional 1.5 TODGA molecules that, on average, coordinate Nd in the bulk organic phase imply that these additional TODGA molecules must add after the final rate limiting step at the interface.

It is possible that TBP is also involved in the mass transfer mechanism based on the observed increase in  $k_{\text{obs}}$  and on the interactions of TBP with the equilibrium species apparent in the absorption spectra. Unfortunately, the kinetic results across TBP concentrations (0.10–1.0 M) were inconclusive (Fig. S1). The apparent TBP reaction orders derived from the TBP data range from 0 to 0.38. Across this range of TBP concentrations, the organic phase bulk and interfacial properties vary significantly due to the PM, which makes it difficult to distinguish between the cosolvent or cosurfactant roles of TBP and its action as an extracting ligand from the apparent reaction order.

For the stripping kinetics (Fig. 9B), 1.0 M TBP in the organic phase slows the rate of stripping significantly over the entire TODGA range. The shape of the  $k_{\text{oa}}$  curve for 1.0 M TBP is significantly altered relative to the curve for the unmodified extraction system, and the 0.25 M TBP data represents a balance between the 1.0 M and unmodified systems. The observed change of shape can arise from multiple effects, but two possibilities seem the most reasonable. One involves a shift of the plateau region to lower TODGA concentrations, which are difficult to monitor with our technique due to the low  $D_{\text{Nd}}$  values. Another possibility is that TBP has changed which steps are rate determining in the reverse mechanism, similar to our observations in the forward direction. An extractant dependence curve that does not plateau and exhibits two distinct linear regions is described by a chemical mechanism for organic  $\rightarrow$  aqueous transfer where the two slowest steps of the sequence are the loss of the final two extractant molecules from the complex.<sup>57</sup> It is difficult to distinguish these possibilities based on the data that we could collect, but molecular dynamics simulations and experiments directed at identifying interfacial speciation may be able to shed light on TBP's impact on the mass transfer.

Solvent extraction equilibrium and kinetic experiments also were performed across a range of equilibrium nitric acid concentrations (0.20–3.0 M  $\text{HNO}_3$ ) at constant concentrations of TODGA and TBP. The results are presented in Fig. 10 using the aqueous nitrate anion activity as the independent variable. Unlike DHOA-modified organic phases, the extraction of  $\text{HNO}_3$  into *n*-dodecane by mixtures of TODGA and TBP has been well characterized by McLachlan *et al.*<sup>45</sup> In order to accurately describe and compare the impact of TBP modification on the equilibrium and kinetics across this acidity range, the distribution ratios ( $D_{\text{Nd}}$ ) were corrected ( $D_{\text{c}}$ ) for the free extractant concentration<sup>45</sup> and the changing activities of water, nitrate anions, and protons in the aqueous phase,<sup>43,44</sup> as explained in the SI. The corrected equilibrium results are displayed in Fig. 10B.

It is evident from the differences between Fig. 10A and B that the corrections for consumption of TODGA by extraction of nitric acid and variations in the aqueous activity coefficients are

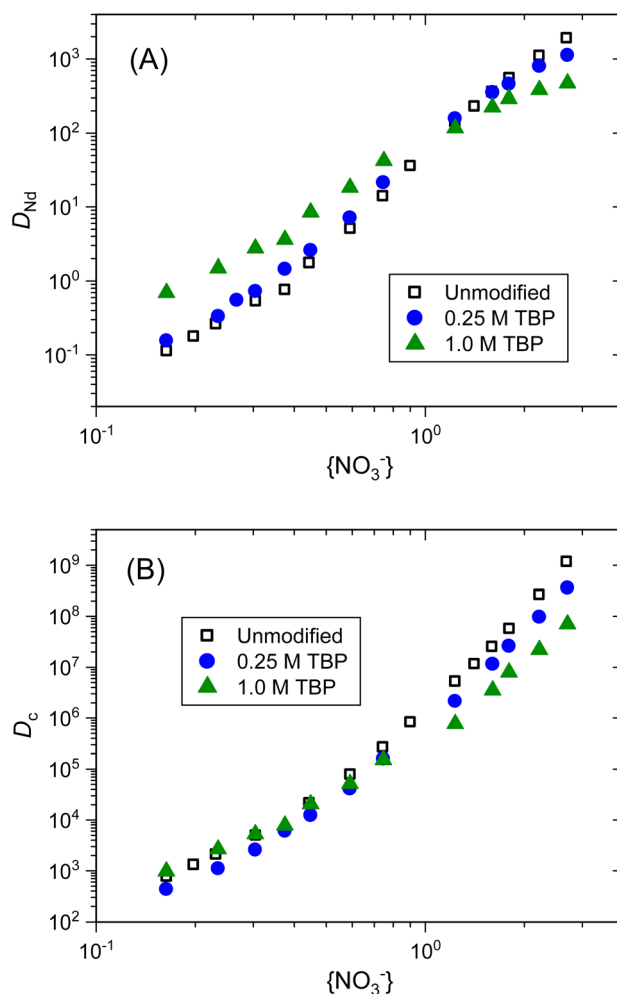


Fig. 10 (A) Experimentally-determined and (B) corrected Nd(III) distribution ratios as a function of nitrate anion activity for the extraction of 4.83 mM Nd(III) from 0.20 to 3.0 M  $\text{HNO}_3$  by 0.10 M TODGA in *n*-dodecane without and with TBP as a phase modifier. No phase modifier (black squares),<sup>37</sup> 0.25 M TBP (blue circles), and 1.0 M TBP (green triangles). Error bars ( $\pm 2\sigma$ ) smaller than the data point have been removed for clarity.

vital to understanding the nitrate dependence across this large range of acidities. Both 0.25 M and 1.0 M TBP led to lower metal extraction for high nitrate activities, with a more pronounced effect when the TBP concentration was quadrupled. As has been observed multiple times for DGA extraction systems, the extraction of trivalent f-element cations at increasing acidities exhibits high nitrate:metal stoichiometries due to the changing speciation in the organic phase.<sup>9,10,59</sup> Despite this curvature, the speciation can be inferred from linear slopes across smaller sections of the data. The apparent nitrate stoichiometries in the extracted complexes at low and high  $\{\text{NO}_3^-\}$  are provided in Table 4. When the nitrate anion activity is low, the unmodified and modified organic phases behave similarly with respect to extracted complexes containing only nitrate species, the three nitrate counteranions required to balance the charge of the Nd(III) cation are accounted for in the data. Across the high  $\{\text{NO}_3^-\}$  region, the presence of TBP lowered the

**Table 4** Slopes of the linear regression fits for the dependence (dep) of  $D_c$  on aqueous nitrate anion activity for unmodified *n*-dodecane<sup>37</sup> and modified with 0.25 M and 1.0 M TBP. Error is reported as  $\pm 2\sigma$  from error-weighted linear regression

Phase modifier	$D_c$ dep across low $\{\text{NO}_3^-\}$	$D_c$ dep across high $\{\text{NO}_3^-\}$
Unmodified	$3.03 \pm 0.08$	$6.91 \pm 0.39$
0.25 M TBP	$2.96 \pm 0.40$	$6.53 \pm 0.10$
1.0 M TBP	$2.71 \pm 0.07$	$5.74 \pm 0.22$

apparent average number of nitrate species coordinated to the equilibrium complexes. From the equilibrium in eqn (6), we can interpret the slopes from Fig. 10B as slope =  $2m + n$ , where  $n = 3$  nitrate anions, and the average number of  $\text{HNO}_3$  adducts is  $m$ . The unmodified organic phase fosters an average of 1.95  $\text{HNO}_3$  adducts in the outer-sphere of the extracted complex at the highest acidities, the presence of 0.25 M TBP lowers the average  $\text{HNO}_3$  stoichiometry to 1.8, while in 1.0 M TBP only an average of 1.4  $\text{HNO}_3$  adducts are associated with the extracted complex.

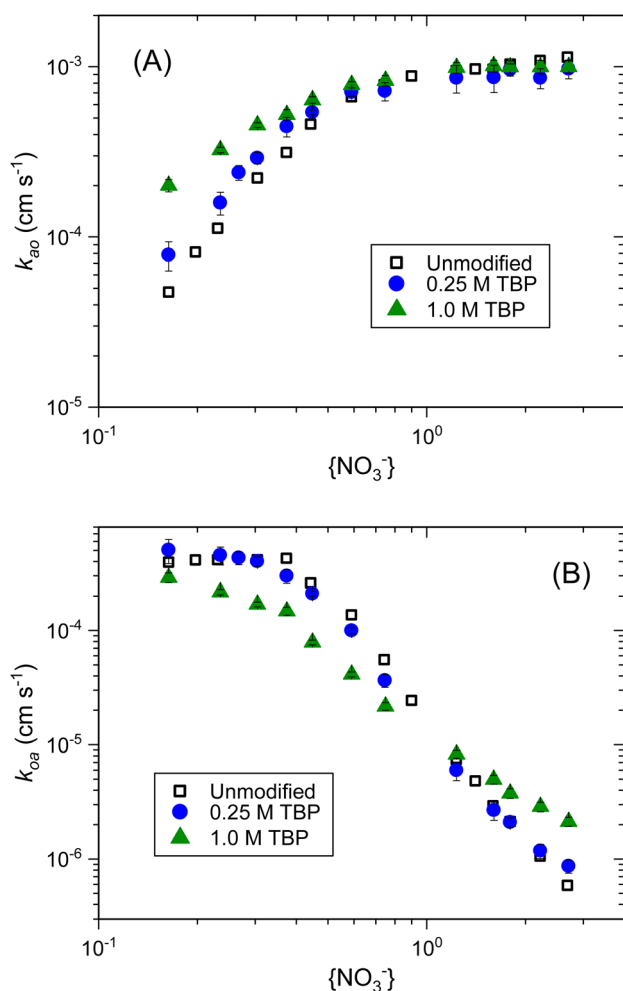


**Fig. 11** Pseudo-first order rate constants for the (A) aqueous to organic and (B) organic to aqueous mass transfer of  $\text{Nd(III)}$  from 0.20 to 3.0 M  $\text{HNO}_3$  by 0.10 M TODGA in *n*-dodecane without and with TBP as a phase modifier. No phase modifier (black squares),<sup>37</sup> 0.25 M TBP (blue circles), and 1.0 M TBP (green triangles). Error bars are provided at  $\pm 2\sigma$ .

In addition to changing the inner coordination of Nd, this shows that TBP affects the outer-sphere  $\text{HNO}_3$  coordination in the TODGA : Nd complexes.

The thermodynamic corrections made to the distribution ratios cannot be reasonably accounted for in the rate constants for mass transfer shown in Fig. 11. Nevertheless, we can draw conclusions from the relationship between  $D_{\text{Nd}}$ ,  $k_{\text{ao}}$ , and  $k_{\text{oa}}$  in eqn (1). Analysis of the 1.0 M TBP modified data reveals that, across low nitrate anion activities, the corrected distribution ratios increased with a slope of approximately 3. In the same region, the changes in  $k_{\text{ao}}$  provide a reaction order of 1.3 with respect to nitrate while changes in  $k_{\text{oa}}$  provide a reaction order of  $-0.8$ . Approximately  $2/3$  of the change in the distribution ratio is accounted for by the changes in  $k_{\text{ao}}$ , while  $1/3$  comes from the changes in  $k_{\text{oa}}$ . Since the equilibrium thermodynamics shows that there are 3 nitrates involved in the partitioning under these conditions, we can interpret these reaction orders to actually represent two nitrate anions as part of the activated complex at the interface in the forward direction, while the third, final nitrate anion associates after the final rate determining step. A charged activated complex is possible owing to the more polar interfacial region provided by the presence of TBP, whose dielectric constant ( $\epsilon$ )<sup>60</sup> is four times greater than that of *n*-dodecane (2).<sup>61</sup>

No plateau region was observed for the reverse rate constants with 1.0 M TBP phase modification, similar to the TODGA dependence data in the 1.0 M TBP system discussed earlier. There appears to be two linear regions, with slopes interpretable through the  $D_c$  slopes given in Table 4. Across the higher nitrate anion activity region, the slope of  $D_c$  is fully accounted for by the changes in  $k_{\text{oa}}$  because of the plateau in the forward extraction rate across the same region. Whether the lack of a plateau in the forward direction means that the plateau has merely shifted to lower nitrate activities or that the rate limiting steps have changed, the plateau in the  $k_{\text{ao}}$  data and the slope of  $D_c$  indicate that the nitrate anions and nitric acid molecules must decomplex before completion of the final slow step in the mass transfer of  $\text{Nd(III)}$  from the organic phase to the aqueous phase.

## Conclusions

Similar to the unmodified TODGA extraction system, organic phases modified by DHOA appear to be governed by an Interfacial Two-Step Consecutive Reactions mechanism, where adsorption and desorption of the metal cation and a metal complex from the interface controls the rates.<sup>55,57</sup> In the DHOA-modified system, three TODGA molecules and three nitrate anions associate with the metal before the desorption of the complex from the interface into the organic phase. In the reverse direction, the  $\text{Nd(TODGA)}_{3,4}(\text{NO}_3)_3(\text{HNO}_3)_{0-2}$  complexes dissociate completely before desorption into the aqueous phase. The equilibrium slope analysis indicates that fewer  $\text{HNO}_3$  adducts are associated with the bulk complex in the 1.0 M DHOA system, and thus fewer  $\text{HNO}_3$  molecules are lost in the stripping mechanism. Confirmation of this finding will require a more detailed treatment of the dependence of  $D_{\text{Nd}}$ ,  $k_{\text{ao}}$ , and  $k_{\text{oa}}$  on the aqueous nitric acid content, which requires a more extensive understanding of the nitric acid



extraction by TODGA + DHOA organic phases. It was determined spectroscopically that DHOA is, for the most part, a non-interacting phase modifier when Nd is extracted, though it may play a solvating role in the outer sphere of the complex. Because of its cosolvent role, the mechanisms and reaction orders are similar to those observed for the unmodified organic phase, except for the interactions with  $\text{HNO}_3$ .

In contrast, phase modification of the TODGA/*n*-dodecane solvent with TBP altered the equilibrium species, the extraction kinetics, and the stripping kinetics of Nd(III) extraction by TODGA. While addition of 0.25 M TBP to the organic phase caused some changes in the system, addition of 1.0 M TBP to TODGA in *n*-dodecane led to sweeping change in both the organic phase and at the interface. TBP was able to displace one TODGA extractant from Nd(III) coordination in the bulk organic solution, which was evident in the equilibrium slope analysis and absorption spectra of Nd(III). TBP also altered the mechanism of mass transfer. When 1.0 M TBP was used, the forward mechanism only involved one TODGA molecule and two nitrate anions in the activated complex. The additional 1.5 TODGA molecules, 1 nitrate anion, and 1.4  $\text{HNO}_3$  adducts add to the complex in fast equilibria after the slow steps of the mechanism. In the reverse kinetics, all the TODGA, nitrate and nitric acid dissociate from the Nd by the final rate-limiting step. The change in the shape of the  $k_{\text{oa}}$  curves across TODGA concentrations and nitrate anion activities potentially indicates that loss of the second-to-last TODGA molecule from the complex is also rate controlling, but further investigations will be needed to verify such a mechanism.

The addition of TBP to *n*-dodecane does far more than just modify the organic phase; it changes the mechanisms of extraction and stripping and encourages lanthanide complexation by TBP in the organic phase. The lack of a significant effect on the equilibrium or kinetics using DHOA and the significant effect using TBP both need to be taken into account when using these modifiers industrially and in future studies.

## Author contributions

Wyatt S. Nobley – conceptualization, formal analysis, investigation, methodology, visualization, writing – original draft, writing – review and editing. Mark P. Jensen – conceptualization, formal analysis, supervision, funding acquisition, visualization, project administration, writing – review and editing.

## Conflicts of interest

There are no conflicts to declare.

## Data availability

Data for this article, including the equilibrium distribution ratios and rate constant data, are given in the supplementary information (SI). Supplementary information is available. See DOI: <https://doi.org/10.1039/d5ra06417a>.

## Acknowledgements

This work was supported by U.S. Department of Energy, Office of Science, Office of Basic Energy Sciences under award DE-SC0022217. The views expressed in the article do not necessarily represent the views of the DOE or the U.S. Government. The U.S. Government retains and the publisher, by accepting the article for publication, acknowledges that the U.S. Government retains a nonexclusive, paid-up, irrevocable, worldwide license to publish or reproduce the published form of this work, or allow others to do so, for U.S. Government purposes.

## References

- 1 D. S. Sholl and R. P. Lively, *Nature*, 2016, **532**, 435–437.
- 2 T. Cheisson and E. J. Schelter, *Science*, 2019, **363**, 489–493.
- 3 A. V. Gelis and G. J. Lumetta, *Ind. Eng. Chem. Res.*, 2014, **53**, 1624–1631.
- 4 K. L. Nash, *Solvent Extr. Ion Exch.*, 2015, **33**, 1–55.
- 5 Y. Sasaki, Y. Sugo, K. Morita and K. L. Nash, *Solvent Extr. Ion Exch.*, 2015, **33**, 625–641.
- 6 P. Tkac, G. F. Vandegrift, G. J. Lumetta and A. V. Gelis, *Ind. Eng. Chem. Res.*, 2012, **51**, 10433–10444.
- 7 T. Sato, *Hydrometallurgy*, 1989, **22**, 121–140.
- 8 D. Stamberg, M. R. Healy, V. S. Bryantsev, C. Albisser, Y. Karslyan, B. Reinhart, A. Paulenova, M. Foster, I. Popovs, K. Lyon, B. A. Moyer and S. Jansone-Popova, *Inorg. Chem.*, 2020, **59**, 17620–17630.
- 9 Y. Sasaki, Y. Sugo, S. Suzuki and S. Tachimori, *Solvent Extr. Ion Exch.*, 2001, **19**, 91–103.
- 10 Y. Sasaki, P. Rapold, M. Arisaka, M. Hirata, T. Kimura, C. Hill and G. Cote, *Solvent Extr. Ion Exch.*, 2007, **25**, 187–204.
- 11 Y. Sasaki, Y. Sugo and S. Tachimori, in *Atalante*, Avignon, 2000, pp. 1–6.
- 12 Y. Sugo, Y. Sasaki and S. Tachimori, *Radiochim. Acta*, 2002, 161–165.
- 13 S. Nave, G. Modolo, C. Madic and F. Testard, *Solvent Extr. Ion Exch.*, 2004, **22**, 527–551.
- 14 R. Chiarizia, K. L. Nash, M. P. Jensen, P. Thiyagarajan and K. C. Littrell, *Langmuir*, 2003, **19**, 9592–9599.
- 15 R. Ganguly, J. N. Sharma and N. Choudhury, *Soft Matter*, 2012, **8**, 1795–1800.
- 16 M. P. Jensen, T. Yaita and R. Chiarizia, *Langmuir*, 2007, **23**, 4765–4774.
- 17 A. A. Peroutka, S. S. Galley and J. C. Shafer, *RSC Adv.*, 2023, **13**, 6017–6026.
- 18 P. Deepika, K. N. Sabharwal, T. G. Srinivasan and P. R. Vasudeva Rao, *Solvent Extr. Ion Exch.*, 2010, **28**, 184–201.
- 19 K. R. Swami, K. A. Venkatesan and M. P. Antony, *Solvent Extr. Ion Exch.*, 2019, **37**, 500–517.
- 20 W. S. Nobley and M. P. Jensen, *Solvent Extr. Ion Exch.*, 2025, **43**, 295–343.
- 21 A. N. Turanov, V. K. Karandashev and M. Boltoeva, *Hydrometallurgy*, 2020, **195**, 1–8.
- 22 D. Woodhead, F. McLachlan, R. Taylor, U. Müllich, A. Geist, A. Wilden and G. Modolo, *Solvent Extr. Ion Exch.*, 2019, **37**, 173–190.



- 23 S. A. Ansari, P. K. Mohapatra and V. K. Manchanda, in *Nuclear and Radiochemistry Symposium (NUCAR 2007)*, 2007, pp. 389–390.
- 24 R. B. Gujar, S. A. Ansari, A. Bhattacharyya, A. S. Kanekar, P. N. Pathak, P. K. Mohapatra and V. K. Manchanda, *Solvent Extr. Ion Exch.*, 2012, **30**, 278–290.
- 25 A. Dhawa, A. Rout, N. R. Jawahar and K. A. Venkatesan, *J. Mol. Liq.*, 2021, **341**, 1–8.
- 26 Y. Sasaki, Z.-X. Zhu, Y. Sugo, H. Suzuki and T. Kimura, *Anal. Sci.*, 2005, **21**, 1171–1175.
- 27 S. Tachimori, Y. Sasaki and S. Suzuki, *Solvent Extr. Ion Exch.*, 2002, **20**, 687–699.
- 28 Y. Sasaki, Y. Sugo, S. Suzuki and T. Kimura, *Anal. Chim. Acta*, 2005, **543**, 31–37.
- 29 K. R. Swami and K. A. Venkatesan, *J. Mol. Liq.*, 2019, **296**, 1–9.
- 30 R. B. Gujar, S. A. Ansari, P. K. Mohapatra and V. K. Manchanda, *Solvent Extr. Ion Exch.*, 2010, **28**, 350–366.
- 31 Z. Chen, X. Yang, L. Song, X. Wang, Q. Xiao, H. Xu, Q. Feng and S. Ding, *Inorg. Chim. Acta*, 2020, **513**, 1–11.
- 32 W.-B. Zhu, G.-A. Ye, F.-F. Li and H.-R. Li, *J. Radioanal. Nucl. Chem.*, 2013, **298**, 1749–1755.
- 33 M. A. Bromley and C. Boxall, *Nukleonika*, 2015, **60**, 859–864.
- 34 M. A. Bromley and C. Boxall, *Prog. Nucl. Sci. Technol.*, 2018, **5**, 70–73.
- 35 T. H. Vu, J.-P. Simonin, A. L. Rollet, R. J. M. Egberink, W. Verboom, M. C. Gullo and A. Casnati, *Ind. Eng. Chem. Res.*, 2020, **59**, 13477–13490.
- 36 X. Liu, X. Huang, Y. Wang, Z. Wang, Q. Yu, H. Zhou, R. Li and S. Ding, *Inorg. Chim. Acta*, 2025, **583**, 122710.
- 37 W. S. Noble, J. J. Klein and M. P. Jensen, *RSC Adv.*, 2025, DOI: [10.1039/d5ra06672g](https://doi.org/10.1039/d5ra06672g).
- 38 K. McCann, S. I. Sinkov, G. J. Lumetta and J. C. Shafer, *New J. Chem.*, 2018, **42**, 5415–5424.
- 39 S. M. Webb, *Phys. Scr.*, 2005, **T115**, 1011–1014.
- 40 J. Jaumot, R. Gargallo, A. De Juan and R. Tauler, *Chemom. Intell. Lab. Syst.*, 2005, **76**, 101–110.
- 41 J. Jaumot, A. de Juan and R. Tauler, *Chemom. Intell. Lab. Syst.*, 2015, **140**, 1–12.
- 42 D. J. Leggett, in *Computational Methods for the Determination of Formation Constants*, ed. D. J. Leggett, Springer US, Boston, MA, 1st edn, 1985, pp. 159–220.
- 43 S. Lalleman, M. Bertrand, E. Plasari, C. Sorel and P. Moisy, *Chem. Eng. Sci.*, 2012, **77**, 189–195.
- 44 A. V. Levanov, O. Y. Isaikina and V. V. Lunin, *Russ. J. Phys. Chem. A*, 2017, **91**, 1221–1228.
- 45 F. McLachlan, K. Greenough, A. Geist, B. McLuckie, G. Modolo, A. Wilden and R. Taylor, *Solvent Extr. Ion Exch.*, 2016, **34**, 334–346.
- 46 D. M. Brigham, A. S. Ivanov, B. A. Moyer, L. H. Delmau, V. S. Bryantsev and R. J. Ellis, *J. Am. Chem. Soc.*, 2017, **139**, 17350–17358.
- 47 A. G. Baldwin, A. S. Ivanov, N. J. Williams, R. J. Ellis, B. A. Moyer, V. S. Bryantsev and J. C. Shafer, *ACS Cent. Sci.*, 2018, **4**, 739–747.
- 48 R. J. Ellis, D. M. Brigham, L. Delmau, A. S. Ivanov, N. J. Williams, M. N. Vo, B. Reinhart, B. A. Moyer and V. S. Bryantsev, *Inorg. Chem.*, 2017, **56**, 1152–1160.
- 49 M. R. Antonio, D. R. McAlister and E. P. Horwitz, *Dalton Trans.*, 2015, **44**, 515–521.
- 50 P. Weßling, U. Müllich, E. Guerinoni, A. Geist and P. J. Panak, *Hydrometallurgy*, 2020, **192**, 1–9.
- 51 E. Campbell, V. E. Holfeltz, G. B. Hall, K. L. Nash, G. J. Lumetta and T. G. Levitskaia, *Solvent Extr. Ion Exch.*, 2018, **36**, 331–346.
- 52 A. A. Peroutka, X. Wang, M. J. Servis and J. C. Shafer, *Inorg. Chem.*, 2024, **63**, 10466–10470.
- 53 A. A. Peroutka, S. S. Galley and J. C. Shafer, *Coord. Chem. Rev.*, 2023, **482**, 1–31.
- 54 T. Prathibha, K. A. Venkatesan and M. P. Antony, *Colloids Surf., A*, 2018, **538**, 651–660.
- 55 P. R. Danesi and G. F. Vandegrift, *J. Phys. Chem.*, 1981, **85**, 3646–3651.
- 56 G. Modolo, H. Asp, C. Schreinemachers and H. Vijgen, *Solvent Extr. Ion Exch.*, 2007, **25**, 703–721.
- 57 P. R. Danesi, R. Chiarizia and C. F. Coleman, *CRC Crit. Rev. Anal. Chem.*, 1980, **10**, 1–126.
- 58 Z. Kolarik and N. Pipkin, *Interfacial Tension in Systems Involving TBP in Dodecane, Nitric Acid, Uranyl Nitrate, and Water*, 1982.
- 59 T. Yaita, A. W. Herlinger, P. Thiyagarajan and M. P. Jensen, *Solvent Extr. Ion Exch.*, 2004, **22**, 553–571.
- 60 M. Yamamoto, *J. Nucl. Sci. Technol.*, 1988, **25**, 540–547.
- 61 Ch. Wohlfarth, *Static Dielectric Constants of Pure Liquids and Binary Liquid Mixtures*, Springer Berlin, Heidelberg, 1st edn, 2008, vol. 27.

